



THE UNIVERSITY *of* EDINBURGH

Edinburgh Research Explorer

The self-referential method combined with thermodynamic integration

Citation for published version:

Sweatman, MB, Atamas, AA & Leyssale, J-M 2008, 'The self-referential method combined with thermodynamic integration', *Journal of Chemical Physics*, vol. 128, no. 6, 064102 .
<https://doi.org/10.1063/1.2839881>

Digital Object Identifier (DOI):

[10.1063/1.2839881](https://doi.org/10.1063/1.2839881)

Link:

[Link to publication record in Edinburgh Research Explorer](#)

Document Version:

Publisher's PDF, also known as Version of record

Published In:

Journal of Chemical Physics

General rights

Copyright for the publications made accessible via the Edinburgh Research Explorer is retained by the author(s) and / or other copyright owners and it is a condition of accessing these publications that users recognise and abide by the legal requirements associated with these rights.

Take down policy

The University of Edinburgh has made every reasonable effort to ensure that Edinburgh Research Explorer content complies with UK legislation. If you believe that the public display of this file breaches copyright please contact openaccess@ed.ac.uk providing details, and we will remove access to the work immediately and investigate your claim.



The self-referential method combined with thermodynamic integration

Martin B. Sweatman,^{a)} Alexander A. Atamas, and Jean-Marc Leyssale

*Department of Chemical and Process Engineering, University of Strathclyde,
Glasgow G1 1XJ, United Kingdom*

(Received 29 October 2007; accepted 14 January 2008; published online 11 February 2008)

The self-referential method [M. B. Sweatman, *Phys. Rev. E* **72**, 016711 (2005)] for calculating the free energy of crystalline solids via molecular simulation is combined with thermodynamic integration to produce a technique that is convenient and efficient. Results are presented for the chemical potential of hard sphere and Lennard-Jones face centered cubic crystals that agree well with this previous work. For the small system sizes studied, this technique is about 100 times more efficient than the parameter hopping technique used previously. © 2008 American Institute of Physics. [DOI: [10.1063/1.2839881](https://doi.org/10.1063/1.2839881)]

I. INTRODUCTION

The crystalline state is fundamental in nature and hugely important in modern technology. Moreover, molecular simulation is increasingly used to understand and predict the properties of matter. Yet, despite this, molecular simulation techniques for classical crystals are, overall, not as satisfactory as those for fluids, and, in particular, there is some confusion in the literature as to how confined crystals can be simulated correctly. Recently, two papers,^{1,2} called papers 1 and 2 here, have made some progress in this area. In paper 1 it was shown how the Gibbs ensemble can be used to simulate coexistence between a crystalline solid phase and another phase without simulating any interface. Central in that work, and to the problem of simulating crystals generally, is calculation of the free energy. This problem was addressed in paper 2.

It is even more important to know the free energy for confined crystals than for confined fluids. This is not just because phase transitions involving crystalline solids are often strongly first order and associated with significant hysteresis—a particular problem with simulations. It is also because we cannot impose or measure the bulk (i.e., experimental) pressure when simulating confined crystals, unless an impractically large system is simulated that includes the confined system—bulk system interface. Instead, it is essential that the chemical potential of the confined crystal is known (imposed or measured) because this quantity is the same in the confined and bulk systems at equilibrium. Unfortunately, we cannot impose the chemical potential on simulated crystals by performing grand-canonical ensemble simulations. The reason for this is explained in detail later. Instead, we should perform simulations that allow the crystal to relax to an equilibrium state, and then seek to measure the chemical potential of the crystal. For crystals confined in uniform slit pores, for example, simulations at constant interfacial tension ($N\sigma T$) are appropriate. For a pure system the chemical potential is then simply the Gibbs free energy

per particle in the $N\sigma T$ ensemble. So for simulation studies of confined crystals calculation of the Gibbs free energy is essential if conditions inside the pore are to be related to experimental (or bulk) conditions, regardless of whether phase behavior is of interest or not. Unfortunately, standard free energy calculation techniques³ for classical crystalline solids are not very satisfactory when applied to confined crystals.

Paper 2 described a radical technique, based on the self-referential (SR) method, for calculating the free energy of crystalline solids. However, as described in more detail below, despite some appealing properties the particular SR technique used in paper 2 was inefficient and not very convenient. For example, one needed to (a) perform two different kinds of special simulation (called “replication” and “relaxation” stages), (b) estimate an initial pressure and temperature, through optimization or trial and error, for the relaxation stage, and (c) use Monte Carlo simulation. This present work resolves all these issues, largely by implementing thermodynamic integration. But before discussing this work, let us turn to the fundamental problem in simulating crystals.

A. The problem with simulating crystals

The following discussion refines arguments put forward in paper 2. We know, by considering density functional theory, for example, that for specified external constraints (temperature, chemical potential, external potential, etc.) that only one “density profile,” or singlet density, represents the equilibrium state. So, for a simulated crystal to reach equilibrium it must be able to adjust its density profile, (provided it is not somehow initiated in this state), i.e., it must be able to adjust its lattice site density, or lattice spacing, in response to external conditions. In grand-canonical simulations^{3,4} volume is fixed and equilibrium is achieved by fluctuations in particle number in response to an applied chemical potential. However, when simulating a space-filling crystal this kind of fluctuation does not lead to a change in the average lattice spacing. It leads only to defects, so it is the wrong kind of fluctuation and hence the system does not achieve equilib-

^{a)}Author to whom correspondence should be addressed. Electronic mail: martin.sweatman@strath.ac.uk.

rium. This happens because of a conflict in symmetry requirements at fixed volume. If the system were fluid instead, i.e., if it did not have crystalline symmetry, then this would not happen—the right kind of fluctuations could occur, even with periodic boundaries, in response to an applied chemical potential. Likewise, if a crystal simulation at fixed volume, somehow, did not employ periodic boundaries then, again, this would not happen—the correct kind of fluctuation could occur in response to an applied chemical potential. So it is the combination of periodic boundaries and crystal symmetry that is the root cause of difficulties when simulating confined crystals at fixed volume.

Of course, for a space-filling crystal fluctuations in individual box lengths can be achieved at fixed volume by shortening one box length while simultaneously lengthening another or by adjusting vertex angles. However, in this case lattice spacing in one direction is traded against another, and although the crystal might be able to relax somewhat, this will still not allow full relaxation to the equilibrium spacing in each direction because these fluctuations do not occur in response to the applied chemical potential. That is, changing the chemical potential will have no significant effect on the system except to alter the density of defects.

The same problem arises with standard Gibbs ensemble simulations^{3,5,6} involving crystalline solids. Once again, the crystalline phase must be able to adjust its average lattice site density so that the chemical potentials of the two simulated phases are equilibrated. Although the lattice spacing can adjust so that pressure is equilibrated, it cannot adjust in response to particle exchanges which are responsible for equilibrating chemical potential. Any particle exchanges that do occur must result in creation or annihilation of defects, which by themselves do not create any change in the average lattice spacing. This problem was resolved in paper 1 by creating a free energy model for the crystal phase. Finally, the same problem also occurs, when the surface area is fixed, for space-filling two-dimensional (2D) crystals (i.e., crystals formed on a surface) and for 2D crystal layers that form on the inner surfaces of a slit pore in contact with a fluid phase that fills the middle of the pore.

Note that the symmetry conflict is not a finite-size effect, i.e., this problem is not automatically resolved by simulating a sufficiently large system because no matter how large the system, one cannot guarantee that it will be initiated with the correct lattice site density, and fluctuations in the lattice spacing cannot usually be made to occur at fixed volume in response to an applied chemical potential. However, a strategy is conceivable that will allow fluctuations in the lattice spacing to occur (at fixed volume) in response to an applied chemical potential. One can imagine a composite Monte Carlo move that simultaneously adjusts crystal lattice spacing, adjusts box lengths in each direction and vertex angles at fixed volume, and adds (or deletes) entire crystal unit cells to the crystal phase. However, we are not aware of any such move applied in the literature—although Tilwani's retiling algorithm⁷ accomplishes a similar feature in the context of Gibbs ensemble simulations of 2D hard disks. Note, however, that this retiling technique cannot be applied to general space-filling three-dimensional crystals because, generally,

single particle number fluctuations would not occur (generally, many particles would simultaneously be created or destroyed in the crystal phase when an entire unit cell is added or deleted), yet the partition function for the grand-canonical and Gibbs ensembles demands single particle fluctuations. So this retiling technique can only be applied correctly for crystals with single particle unit cells.

Of course, another problem when simulating dense phases has to do with the probability of acceptance of insertion and deletion moves, but this is only a practical problem that might be tackled with sufficient computing resources or clever algorithms.³ The problem concerning the lattice site density is more fundamental.

Despite all this, there are several examples⁸⁻¹⁵ in the literature where the grand-canonical ensemble has been used to simulate space-filling crystalline solids and 2D crystals on the inner surfaces of slit pores without box length fluctuations. All this work should be considered carefully because in every case these are not equilibrium simulations. So the stated location of fluid-crystal phase transitions for bulk and confined systems might not be precisely correct. In much of this work a “Landau free energy” method is used which gradually transforms a liquid phase into a crystal phase using biased sampling. Although the liquid phase end point of these simulations is in equilibrium with the imposed chemical potential, the crystal phase end point is not because the crystal density is also influenced by the size and shape of the simulation box, which is fixed arbitrarily in advance. Without further studies it is not possible to quantify the systematic error introduced by this technique; it will be different for each case. Note also the simulations by Dominguez *et al.*¹⁶ in which crystalline solid free energies for a slit-pore system are calculated using an ensemble in which the slit-pore area is fixed, while fluctuations are allowed in slit width in response to the fixed condition of transverse pore pressure. Once again, these are not equilibrium simulations because the lattice site density cannot adjust to the imposed condition of fixed transverse pressure, i.e., the chemical potential of their crystal will generally not correspond to the bulk (reservoir) chemical potential corresponding to the imposed transverse pressure. We can expect that their free energy calculations and hence their predicted phase transition points are dependent on their choice of slit-pore area (i.e., their choice of initial lattice site density).

B. The self-referential method

The aim of this present work is to develop a novel simulation technique, based on the self-referential method, for calculating the free energy of crystalline solids that is convenient and efficient. For the purpose of validation, we demonstrate this technique using the same simple crystals as in paper 2. Future work will aim to demonstrate that the self-referential method is also versatile and robust by application to molecular crystals. Ultimately, we aim to apply this technique to confined crystals so that the problems discussed above might be resolved.

All simulation methods^{3,17-25} that calculate free energies for crystals actually calculate the free energy difference be-

tween the state of interest and a reference state for which the free energy is known. The self-referential technique² is interesting because it takes the crystalline solid of interest as the reference state. So the only difference between the state of interest and the reference state is their size—the reference state has fewer unit cells. This has many advantages when compared to other techniques. Other techniques use a constrained ideal gas (the single-occupancy cell method of Ree and Hoover²⁶), a liquid (the phase switching method of Wilding and Bruce²² calculates the free energy difference between liquid and crystalline solid states, so if the liquid free energy is known it can be used to calculate the absolute free energy of the solid), or an ideal crystal (the various techniques of Frenkel and Ladd²⁰ and Meijer *et al.*²⁷ use an Einstein crystal). All of these techniques require integration of the free energy along a path that connects the reference state with the state of interest. Because the reference state is rather different to the state of interest this can be inconvenient, and sometimes problematic. However, no such integration problems are encountered with the self-referential technique. With this technique only the crystal state of interest, at the density of interest, is simulated. This means that this technique has the potential to be the most convenient, versatile, and efficient technique yet devised.

In paper 2 this idea was applied to simulate some simple crystals using a specialized isothermal-isobaric ensemble Monte Carlo technique to calculate the Gibbs free energy. In earlier work²⁸ Barnes and Kofke simulated one-dimensional hard rods within the canonical ensemble. They calculated the Helmholtz free energy for this system by system-size doubling (using an altogether different technique to the one described in paper 2), and compared their results with exact values for the grand-canonical Helmholtz free energy. Even though the canonical ensemble is not extensive, they obtained good agreement indicating that their system was sufficiently large. They coined the phrase “self-referential” for this general idea. A somewhat similar approach was used by Mon²⁹ and Mon and Binder.³⁰ They calculated the free energy difference between lattice systems (once again in the canonical ensemble) that are identical except for their size. However, in this particular work scaling of the free energy with system size is explicitly not assumed, and so this approach should not be considered to be of the SR kind.

Strictly, for general systems, we should choose to use an ensemble where the free energy actually does scale linearly with size for all system sizes (ignoring periodic boundary induced finite-size effects). In paper 2 the isothermal-isobaric ensemble (*NPT*) was used, for which the Gibbs free energy does scale with system size. If the small system has n_s unit cells and the large one has n_l , then the free energy per unit cell of this structure is $\Delta G/(n_l - n_s)$, where ΔG is the Gibbs free energy difference between these two systems. For a pure crystal the chemical potential $\mu = \Delta G/N_c(n_l - n_s)$, where N_c is the number of particles per unit cell. For a mixture we must also know the difference in chemical potential between each species to obtain the absolute chemical potentials. For alloys, this problem might be resolved using a semigrand ensemble simulation.^{3,31}

The SR method has two stages: A replication stage fol-

lowed by a relaxation stage. If the large system is twice the size of the small system, as is the case in paper 2, then starting with a single-size system, replication produces a double-size system that is constrained such that it is almost exactly self-similar, i.e., the newly created half of the double-size crystal has coordinates almost identical, to within a tolerance, to the original single-size crystal. Relaxation gradually relaxes this self-similarity constraint until the constraint no longer has any effect on the crystal. The resulting double-size crystal has twice the Gibbs free energy of the original single-size crystal. The replication stage is needed because the probability of creating an unconstrained double-size system immediately from a single-size system is vanishingly small. The relaxation stage is then needed to relax the constrained double-size crystal.

It is useful to maintain the constrained double-size crystal at a density similar to the single-size crystal for two reasons. First, so that it is not affected by phase transitions. And second, so that the relaxation simulations can be performed with a single efficient choice of Monte Carlo move parameters. To achieve this, the pressure and temperature of the constrained double-size system can be changed. In paper 2 the initial pressure and temperature of this system were determined by trial and error. But this is inconvenient. It would be much better if the initial pressure and temperature of the constrained double-size system could be determined immediately. This present work shows that, in fact, a good choice is always to set the initial temperature of the constrained double-size system to be twice that of the single-size system and to leave the pressure unchanged. This is a similar conclusion to that of Barnes and Kofke²⁸ who worked in the canonical ensemble and also suggested the initial temperature of the constrained double-size system should be twice that of the single-size system.

In paper 2 the free energy differences for the replication and relaxation stages were calculated using “parameter hopping.”³² This technique simulates two neighboring states (defined by nearly identical parameters) simultaneously, allowing transitions back and forth between them. The free energy difference between these neighboring states is then simply related to their relative probability of occurrence. However, this technique is inconvenient and inefficient. It is inconvenient for two reasons. First, two different and special kinds of simulation are needed; replication and relaxation simulations. Second, only Monte Carlo simulation can be used. It is inefficient because typically thousands of individual parameter hops, each of which corresponds to a simulation, are needed to traverse the large free energy difference between constrained and unconstrained double-size systems. This present work shows how the replication simulation can be replaced by an ordinary simulation of the single-size system provided the initial temperature and pressure of the constrained double-size system are chosen as described above, and how a thermodynamic integration technique can be used instead of parameter hopping to improve the efficiency of the relaxation stage by about two orders of magnitude, depending on the system size. These changes also allow molecular dynamics, at least in principle, to be used.

Finally, in paper 2 the initial “tolerance,” or self-

similarity constraint of the double-size system, is determined, in that case by trial and error, such that the initial constrained double-size system can be generated with reasonable probability. This present work shows how this inconvenience is avoided, and how to determine whether the integration limits (both upper and lower) for the relaxation stage are sufficient. Overall, the resulting SR method is now convenient and efficient.

The following sections describe the SR method and the thermodynamic integration technique used here in detail, and present results for hard-sphere and Lennard-Jones face-centred-cubic crystals that are in excellent agreement with paper 2. We conclude with a summary.

II. THE SR METHOD WITH THERMODYNAMIC INTEGRATION

We work initially with the isothermal-isobaric ensemble, but later also present the corresponding equations for the canonical ensemble and show how results can be converted between ensembles. Periodic boundaries are assumed. We consider only spherical particles, and perfect pure crystals.

A. Replication

First, let us consider the replication stage. Here we wish to find the free energy difference between a single-size system and a constrained, nearly self-similar, double-size system. Actually, for convenience we calculate

$$\Delta(\beta G_{\text{rep}}) = \frac{G_{\alpha_1}}{k_B T_{\alpha_1}} - \frac{G_s}{k_B T_s}, \quad (1)$$

where G is the Gibbs free energy, $\beta^1 = k_B T$ (k_B is Boltzmann's constant and T is temperature), and subscripts s and α_1 indicate the single-size and initial constrained double-size systems.

This can be achieved by analyzing the relevant partition functions Φ because $G = -k_B T \ln \Phi$. The single-size partition function for spherical particles is

$$\Phi_s = \Lambda_s^{-3N_s} \int_0^\infty dV_s \exp(-\beta_s P_s V_s) \frac{1}{N_s} \int_{V'} d\mathbf{r}^{N_s} \times \exp(-\beta_s U_s(\mathbf{r}^{N_s})). \quad (2)$$

Here, Λ^{-3N} represents integration over momentum degrees of freedom, which can be performed independently (Λ has units of length). The contribution of this factor is known exactly, so we will omit all such factors and concentrate on the configurational contribution. P , V , and N are the pressure, volume, and number of particles, respectively. Position coordinates for N particles are denoted $\mathbf{r}^N = \mathbf{r}_1 \mathbf{r}_2 \cdots \mathbf{r}_N$, and the V' symbol indicates that particle positions are not permuted, hence the factor N in the denominator rather than the usual $N!$. U is the configurational contribution to the Hamiltonian, i.e., the interaction energy. By clamping particle 1 to a fixed position, and by dropping factors of Λ , we obtain

$$\Phi_s = \int_0^\infty dV_s \exp(-\beta_s P_s V_s) \frac{V_s}{N_s} \int_{V'} d\mathbf{r}^{N_s-1} \times \exp(-\beta_s U_s(\mathbf{r}^{N_s})), \quad (3)$$

where a factor V_s replaces $\int_{V'} d\mathbf{r}_1$.

Likewise, the partition function of the constrained double-size crystal is

$$\Phi_\alpha = \int_0^\infty dV_d \exp(-\beta_\alpha P_\alpha V_d) \frac{V_d}{N_d} \int_{V'} d\mathbf{r}^{N_d-1} \times \exp(-\beta_\alpha U_\alpha(\mathbf{r}^{N_d})). \quad (4)$$

Here, quantities which can depend on the tolerance constraint α of the double-size system have the subscript α , while quantities which are independent of the tolerance constraint have the subscript d . The configurational contribution to the Hamiltonian of the double-size system includes the self-similarity constraint, which is a function of the tolerance α , and is written

$$U_\alpha(\mathbf{r}^{N_d}) = U_s(\mathbf{r}^{N_d}) + \sum_{j=1}^{N_s} \phi(|\mathbf{r}_{j+N_s} - \mathbf{r}_j - \mathbf{L}_x| - \alpha L_x), \quad (5)$$

where the tolerance constraint is the infinite step function,

$$\phi(r) = \begin{cases} \infty, & r > 0 \\ 0, & r \leq 0, \end{cases} \quad (6)$$

L_x is the length of the vector \mathbf{L}_x that defines the x -vertex of half the double-size system simulation box, and \mathbf{r}_j is the position coordinates of the j th particle. Clearly, according to these equations the double-size system simulation box is twice as long as the single-size system in the x direction.

For the initial, fully constrained double-size system we have

$$\Phi_{\alpha_1} = \int_0^\infty dV_d \exp(-\beta_{\alpha_1} P_{\alpha_1} V_d) \frac{V_d}{N_d} \int_{V'} d\mathbf{r}^{N_d-1} \times \exp(-\beta_{\alpha_1} U_{\alpha_1}(\mathbf{r}^{N_d})). \quad (7)$$

This can be approximated as

$$\Phi_{\alpha_1} \approx 2 \int_0^\infty dV_s \exp(-2\beta_{\alpha_1} P_{\alpha_1} V_s) \frac{V_s}{N_s} \int_{V'} d\mathbf{r}^{N_s-1} \times \exp(-2\beta_{\alpha_1} U_s(\mathbf{r}^{N_s})) \nu_{\alpha_1}^{N_s}, \quad (8)$$

where $\nu_{\alpha_1} = 4\pi(\alpha_1 L_x)^3/3$ is the volume available to a particle in the replicated half of the crystal when $\alpha = \alpha_1$. This approximation is exact in the limit $\alpha_1 \rightarrow 0$.

By choosing $P_{\alpha_1} = P_s$ and $\beta_{\alpha_1} = \beta_s/2$ we obtain

$$\Phi_{\alpha_1} \approx 2 \int_0^\infty dV_s \exp(-\beta_s P_s V_s) \frac{V_s}{N_s} \int_{V'} d\mathbf{r}^{N_s-1} \times \exp(-\beta_s U_s(\mathbf{r}^{N_s})) \nu_{\alpha_1}^{N_s}. \quad (9)$$

So, we immediately see that

$$\Delta(\beta G_{\text{rep}}) = -\ln\left(\frac{\Phi_{\alpha_1}}{\Phi_s}\right) \approx -N_s \ln\langle v_{\alpha_1} \rangle_s - \ln(2), \quad (10)$$

where the angle brackets denote an ensemble average. This relation, which becomes exact in the limit $\alpha_1 \rightarrow 0$, is useful because it allows the special Monte Carlo replication stage simulation described in paper 2 to be replaced by an ordinary (Monte Carlo or molecular dynamics) simulation of the single-size system. It is also much more convenient because P_{α_1} and β_{α_1} are automatically determined, rather than found through some complicated optimization or trial-and-error procedure. For crystals with cubic unit cells we have $\langle v_{\alpha_1} \rangle_s = 4\pi\alpha_1^3 \langle V_s \rangle_s / 3$, which is easily measured provided α_1 is known.

B. Relaxation

The relaxation stage calculates

$$\Delta(\beta G_{\text{rel}}) = \frac{G_{\alpha_m}}{k_B T_s} - \frac{G_{\alpha_1}}{k_B T_{\alpha_1}} = \frac{2G_s}{k_B T_s} - \frac{G_{\alpha_1}}{k_B T_{\alpha_1}}, \quad (11)$$

where subscript α_m indicates the largest constraint used. This should be chosen such that increasing it has no effect on the double-size system. Clearly,

$$G_s = \beta_s^{-1} (\Delta(\beta G_{\text{rep}}) + \Delta(\beta G_{\text{rel}})). \quad (12)$$

Paper 2 uses parameter hopping to calculate this difference, i.e., $\Delta(\beta G_{\text{rel}}) = \sum_{i=1}^{m-1} \Delta(\beta G)_i$, where m is rather large, typically several thousand. As discussed earlier, this is not efficient, and the use of parameter hopping requires Monte Carlo simulation. The main aim of this present work is to develop an efficient and convenient thermodynamic integration technique to achieve this calculation, i.e., to evaluate

$$\Delta(\beta G_{\text{rel}}) = \int_{\alpha_1}^{\alpha_m} d\alpha \frac{d(\beta G)_\alpha}{d\alpha}. \quad (13)$$

To calculate $d(\beta G)_\alpha/d\alpha$ we remember that $\beta G = -\ln \Phi$, and hence

$$\begin{aligned} \frac{d(\beta G)_\alpha}{d\alpha} &= -\frac{1}{\Phi_\alpha} \frac{d\Phi_\alpha}{d\alpha} = \left\langle \left\langle (P_s V_\alpha + U_\alpha) \frac{\partial \beta_\alpha}{\partial \alpha} \right\rangle_\alpha \right. \\ &\quad \left. + \left\langle \beta_\alpha \frac{\partial U_\alpha}{\partial \alpha} \right\rangle_\alpha \right\rangle. \end{aligned} \quad (14)$$

So we have two contributions to $\Delta(\beta G_{\text{rel}})$; one due to changes in temperature,

$$\Delta(\beta G_T) = \int_{\beta_s/2}^{\beta_s} d\beta \langle P_s V_\alpha + U_\alpha \rangle_\alpha, \quad (15)$$

and one due to changes in the tolerance constraint,

$$\Delta(\beta G_g) = \int_{\alpha_1}^{\alpha_m} d\alpha \left\langle \beta_\alpha \frac{\partial U_\alpha}{\partial \alpha} \right\rangle_\alpha. \quad (16)$$

The former is easily determined by a series of simulations and quadrature, provided the β -path is known. In paper 2 a simple algorithm was suggested capable of choosing the β -path so that the density remains reasonably constant over

the range of β . In this present work we use a similar algorithm, to which we turn later. To determine the latter contribution we must first differentiate the configurational contribution to the Hamiltonian with respect to α . To achieve this we prefer instead to work with the configurational contribution defined by

$$U_\alpha(\mathbf{r}^{N_d}) = U_s(\mathbf{r}^{N_d}) + \gamma \sum_{l=1}^{N_s} \Theta(r'_l - \alpha L_x)(r'_l - \alpha L_x), \quad (17)$$

where $r'_l = |\mathbf{r}_{i+N_s} - \mathbf{r}_i - \mathbf{L}_x|$, Θ is the Heaviside step function, and γ is an arbitrary constant. This expression is identical to Eq. (5) in the limit $\gamma \rightarrow \infty$. So, we will work with this expression, and finally take the limit $\gamma \rightarrow \infty$ to obtain the desired result. We now find

$$\frac{\partial U_\alpha}{\partial \alpha} = -\gamma L_x \sum_{i=1}^{N_s} (\delta(r'_i - \alpha L_x)(r'_i - \alpha L_x) + \Theta(r'_i - \alpha L_x)). \quad (18)$$

So, we need to calculate

$$\begin{aligned} \Delta(\beta G_g) &= \int_{\alpha_1}^{\alpha_m} d\alpha \left\langle -\beta_\alpha \gamma L_x \sum_{i=1}^{N_s} (\delta(r'_i - \alpha L_x)(r'_i - \alpha L_x) \right. \\ &\quad \left. + \Theta(r'_i - \alpha L_x)) \right\rangle_\alpha. \end{aligned} \quad (19)$$

The first term in the brackets is always zero, and the remainder can be written

$$\begin{aligned} \Delta(\beta G_g) &= -4\pi N_s \gamma \int_{\alpha_1}^{\alpha_m} d\alpha \beta_\alpha \int_0^\infty dL_x p_\alpha(L_x) L_x \\ &\quad \times \int_0^\infty dr'_i (r'_i)^2 g_\alpha(r'_i, L_x) \Theta(r'_i - \alpha L_x), \end{aligned} \quad (20)$$

where $g_\alpha(r'_i, L_x)$ is the probability distribution function (rather like a radial distribution function) for r'_i when the tolerance is α and the half box x -length is L_x , and $p_\alpha(L_x)$ is the probability distribution for L_x when the tolerance is α . This reduces to

$$\begin{aligned} \Delta(\beta G_g) &= -4\pi N_s \gamma \int_{\alpha_1}^{\alpha_m} d\alpha \beta_\alpha \int_0^\infty dL_x p_\alpha(L_x) L_x \\ &\quad \times \int_{\alpha L_x}^\infty dr'_i (r'_i)^2 g_\alpha(r'_i, L_x). \end{aligned} \quad (21)$$

We can now take the limit $\gamma \rightarrow \infty$ as follows. First, we note that in this limit

$$g_\alpha(r'_i, L_x) = g_\alpha(\alpha L_x, L_x) \exp(-\beta_\alpha \gamma (r'_i - \alpha L_x)), \quad (22)$$

$$r'_i \geq \alpha L_x.$$

We obtain this expression as follows. Because the Hamiltonian involves a piecewise continuous tolerance constraint this pair distribution function for $r'_i \geq \alpha L_x$ is given by

$$g_\alpha(r'_i, L_x) = g_\alpha(\alpha L_x, L_x) \exp(-\beta_\alpha \gamma (r'_i - \alpha L_x) + c_\alpha(r'_i, L_x) - c_\alpha(\alpha L_x, L_c)), \quad r'_i \geq \alpha L_x, \quad (23)$$

where c_α represents the effective potential resulting from indirect interactions, or correlations, between a particle and its constrained partner. As $\gamma \rightarrow \infty$ the constraint potential dominates this expression because it becomes increasingly strong and short ranged. So as $\gamma \rightarrow \infty$, c_α becomes essentially constant over that part of g_α that is not effectively zero. Inserting Eq. (22) into Eq. (21) gives

$$\begin{aligned} \Delta(\beta G_g) &= -4\pi N_s \gamma \int_{\alpha_1}^{\alpha_m} d\alpha \beta_\alpha \int_0^\infty dL_x p_\alpha(L_x) L_x \\ &\times \int_{\alpha L_s}^\infty dr'_i (r'_i)^2 g_\alpha(\alpha L_x, L_x) \\ &\times \exp(-\beta \gamma (r'_i - \alpha L_x)), \end{aligned} \quad (24)$$

which can be integrated, and the limit taken, to give

$$\Delta(\beta G_g) = -4\pi N_s \int_{\alpha_1}^{\alpha_m} d\alpha \int_0^\infty dL_x p_\alpha(L_x) g_\alpha(\alpha L_x, L_x) \alpha^2 L_x^3. \quad (25)$$

However, in the limit $\alpha_1 \rightarrow 0$, we find that $4\pi g_\alpha \alpha^2 L_x^3 / 3 = 1/\alpha$, and so greater numerical accuracy is achieved by integrating with respect to $\ln(\alpha)$. This transforms Eq. (25) to

$$\begin{aligned} \Delta(\beta G_g) &= -4\pi N_s \int_{\ln(\alpha_1)}^{\ln(\alpha_m)} d \ln \alpha \\ &\times \int_0^\infty dL_x p_\alpha(L_x) g_\alpha(\alpha L_x, L_x) \alpha^3 L_x^3. \end{aligned} \quad (26)$$

Finally, it is convenient to write this as

$$\Delta(\beta G_g) = -4\pi N_s \int_{\ln(\alpha_1)}^{\ln(\alpha_m)} d \ln \alpha \{g_\alpha(\alpha L_x, L_x) \alpha^3 L_x^3\}_\alpha, \quad (27)$$

where the curly brackets denote an ensemble average with respect to L_x .

Putting Eqs. (10), (15), and (27) together gives our final result for the configurational contribution, which in terms of a length scale λ is

$$\begin{aligned} \Delta(\beta G) &\cong -N_s \ln \left\langle \frac{v_{\alpha_1}}{\lambda^3} \right\rangle_s - \ln(2) \\ &+ \int_{\beta_s/2}^{\beta_s} d\beta \langle P_s V_\alpha + U_\alpha \rangle_\alpha - 4\pi N_s \\ &\times \int_{\ln(\alpha_1)}^{\ln(\alpha_m)} d \ln \alpha \{g_\alpha(\alpha L_x, L_x) \alpha^3 L_x^3\}_\alpha, \end{aligned} \quad (28)$$

which is exact in the limits $\alpha_1 \rightarrow 0$ and $\alpha_m \rightarrow \infty$. The momentum contribution in terms of this length scale is $3N_s \ln(\Lambda_s/\lambda)$. Note that this length scale factor was implied, but not explained, in paper 2. Also note that for hard spheres $U_\alpha = 0$. The factor $\ln(2)$ in Eq. (28) also deserves some discussion. We know that the Gibbs free energy is perfectly extensive, and so is proportional to N_s . The only term in Eq.

(28) that appears not to be extensive is this $\ln(2)$ factor. It originates from our use of clamping; if we did not clamp particle 1 then this factor would vanish. So it is an artifact of our technique, and will be compensated by an opposite factor of $\ln(2)$ that is “buried” within the ensemble averages in Eq. (28). In other words, these ensemble averages are not actually perfectly extensive because of this $\ln(2)$ factor.

This expression depends only on the tolerance constraint limits, α_1 and α_m . In principle it should be independent of the β -path taken during the relaxation stage, provided the crystal does not undergo any change of phase. To this end, it is important that β be manipulated as α changes during the relaxation stage so that no phase changes can occur. For example, the crystal should not melt. We use a similar algorithm as in earlier work to achieve this. So, first a target volume is defined for the double-size system, $V_t = 2\langle V_s \rangle_s$, where $\langle V_s \rangle_s$ is obtained from the same single-size simulation needed to obtain $\langle v_{\alpha_1} \rangle_s$. A series of simulations are performed where α_i is the value of α for the i th simulation. An index k_v is set to zero initially and if $\langle V_{\alpha_i} \rangle_{\alpha_i} < V_t$ for any simulation; otherwise it is incremented by 1. Changes in β are chosen according to

$$\beta_{\alpha_i} = \beta_{\alpha_{i-1}} + \begin{cases} \frac{\beta_s - \beta_{\alpha_{i-1}}}{m-i} \min(k_v, m-i), & 1 < i < m \\ \beta_s - \beta_{\alpha_{i-1}}, & i = m, \end{cases} \quad (29)$$

α_m and α_1 can be decided by analyzing $\{g_\alpha(\alpha L_x, L_x)\}_\alpha$. α_m is large enough when $\{g_{\alpha_m}(\alpha_m L_x, L_x)\}_{\alpha_m} \cong 0$, and small enough when $\{g_{\alpha_1}(r'_i, L_x)\}_{\alpha_1} \cong \langle 1/v_{\alpha_1} \rangle_{\alpha_1}$ since then the approximation (8) is accurate.

The corresponding canonical ensemble result for the change in the configurational contribution to the Helmholtz free energy is simply

$$\begin{aligned} \Delta(\beta F) &\cong -N_s \ln \left(\frac{v_{\alpha_1}}{\lambda^3} \right) + \int_{\beta_s/2}^{\beta_s} d\beta \langle U_\alpha \rangle_\alpha \\ &- 4\pi N_s \int_{\ln(\alpha_1)}^{\ln(\alpha_m)} d \ln(\alpha) g_\alpha(\alpha L_x, L_x) \alpha^3 L_x^3. \end{aligned} \quad (30)$$

With this ensemble there are no volume fluctuations and so the β -path can be taken to be linear with α , resulting in a straightforward and efficient calculation for the free energy difference, which will depend on the *volume* of the ensemble, i.e., $\Delta F(V)$. Note also that the $\ln(2)$ term in Eq. (28) does not appear here. Again, this is a result of clamping. If we did not clamp particle 1 then the $\ln(2)$ term would be present in Eq. (30).

The Gibbs free energy or chemical potential corresponding to a given pressure can be obtained from this canonical ensemble calculation provided it is sufficiently large that finite-size errors are insignificant. Then we can approximate $F(V) = \Delta F(V)$ and use the reverse of a technique suggested in paper 1 (note there is a sign error in paper 1). So, if an additional isothermal-isobaric simulation is performed, and the volume probability distribution function of this simulation, $p(V)$, is measured, then we have

TABLE I. Results for the SR method with parameter hopping for 108 hard spheres at $\beta P^*=11.48724$, $\alpha_1=0.0002164$, and $\alpha_m=0.17037$. $n_\alpha-1$ is the number of integration steps, and the total number of MC attempts includes the replication and relaxation stage simulations. Error estimates are to 1 standard deviation. Simulations are performed on a standard 3.0 Ghz desktop personal computer.

n_α	Total MC attempts (10^6)	$\beta\mu_{\text{rep}}$	$\beta\mu_{\text{rel}}$	$\beta\mu$	Time (s)
2500	9350	1.2323 ± 0.0011	14.785 ± 0.012	16.017 ± 0.012	34569

$$G = \mu N = k_B T \ln p(V) + F(V) + PV. \quad (31)$$

This shows that the free energy (and chemical potential) at a given *pressure* can be calculated from the free energy at a particular volume (and the same temperature), provided the volume probability distribution function at the given pressure and temperature is known. This route to the Gibbs free energy or chemical potential is no more complicated than via Eq. (28) because both routes require an isothermal-isobaric simulation of the single-size system in addition to the relaxation simulations. The accuracy, and hence efficiency, of each route will depend on how well volume fluctuations are sampled in each case. We expect a similar level of numerical effort for each route will achieve a similar level of accuracy. In this work we adopt the isothermal-isobaric route [Eq. (28)] so that results can be compared directly with those in paper 2. This also avoids the approximation $F(V)=\Delta F(V)$. However, if the effect of finite-size systems is to be investigated, as is usually the case, it should be more efficient to perform canonical ensemble simulations for all system sizes, and to convert to the isothermal-isobaric ensemble using only a simulation of the largest system studied. This route would also be slightly more straightforward because the temperature change algorithm [Eq. (29)] need not be used.

C. Numerical and simulation details

Equation (28) requires two kinds of simulation. First, an ordinary isothermal-isobaric simulation of the single-size system to evaluate $\langle \nu_{\alpha_1} \rangle_s$. The integrals in Eq. (28) are carried out numerically using the trapezium rule. This requires n_α separate evaluations of $\langle P_s V_\alpha + U_\alpha \rangle_\alpha$ and $\{g_\alpha(\alpha L_x) \alpha^3 L_x^3\}_\alpha$, each with a different value of α . We choose to start with α_1 , and increment α such that $d(\ln \alpha) = \chi$ is constant [so $(\ln(\alpha_m/\alpha_1))/(n_\alpha-1) = \chi$]. Each ensemble average is calculated using Monte Carlo simulation with the Hamiltonian in Eq. (5). $\langle V_\alpha \rangle_\alpha$ and $\langle U_\alpha \rangle_\alpha$ are straightforward ensemble averages. We divide $\{g_\alpha(r'_{ij}) \alpha^3 L_x^3\}_\alpha$ into n_b bins and calculate $\{g_\alpha(\alpha L_x) \alpha^3 L_x^3\}_\alpha$ by linear extrapolation to $r'_{ij} = \alpha L_x$ using the ensemble averages of the n_b th and n_{b-1} th bins.

There are four sources of systematic error determined by the choice of α_1 , α_m , n_α , and n_b . These systematic errors can always be reduced below any statistical error by reducing α_1 , and/or increasing α_m , n_α , and n_b . Statistical errors are estimated using a block-averaging method.³³

To improve efficiency, simulations of the double-size constrained systems involve compound translation moves. These are described in detail in paper 2, and involve attempts to move a particle and its constrained partner simultaneously as follows. Both particles are moved by the same amount $\delta \mathbf{r}$,

which is chosen as per the usual displacement selection criteria for particles in the small system. Then one of the particles, labeled j or $j+N_s$ chosen randomly with equal probability, is displaced by a further amount $\delta \mathbf{r}'$. The maximum displacement allowed for $\delta \mathbf{r}'$ is the minimum of the maximum displacement allowed for $\delta \mathbf{r}$ and the tolerance constraint αL_x . Volume scaling moves are also described in detail in paper 2. Note that the tolerance constraint scales with system volume through Eq. (5). Finally, each simulation is suitably equilibrated before statistics are measured.

To compare numerical efficiency, code for the parameter hopping method of paper 2 has been rewritten using as many of the subroutines developed for the thermodynamic integration technique described above as possible. This revealed two errors in certain aspects of the results of paper 2, although the final results quoted in paper 2 are valid. First, there is a systematic error (resulting from incorrect clamping of particle 1) which is significant compared to the statistical error quoted for μ_0 in paper 1, but much less than the statistical error quoted for μ_m . Second, an error was made in reporting T_{d1} for the Lennard-Jones (LJ) system in paper 2. Consequently, this work provides new results for the parameter hopping technique using this new code.

III. RESULTS FOR SIMPLE SYSTEMS

As with paper 2, the aim of this present work is to test and validate the self-referential method, this time using the thermodynamic integration technique described above. The same simple model crystals are used here so that results can be compared with those in paper 2. The hard sphere and shifted-force LJ potentials are pair potentials, so

$$U_s(\mathbf{r}^{N_d}) = \sum_{j>i=1}^{N_d} \varphi(|\mathbf{r}_i - \mathbf{r}_j|), \quad (32)$$

where for hard spheres of diameter d

$$\varphi(r) = \begin{cases} \infty, & r \leq d \\ 0, & r > d, \end{cases} \quad (33)$$

while for the shifted-force LJ potential it is

$$\varphi(r) = \begin{cases} \varphi_{\text{LJ}}(r) - \varphi_{\text{LJ}}(r_c) - \varphi'_{\text{LJ}}(r_c), & r \leq r_c \\ 0, & r > r_c. \end{cases} \quad (34)$$

Here, $\varphi_{\text{LJ}}(r) = 4\epsilon(x^{12} - x^6)$ is the full LJ potential, ϵ is the LJ energy parameter, $x = \sigma/r$, where σ is the LJ length parameter, r_c is the cutoff range (2.5σ in this case), and the dash indicates differentiation with respect to the separation r . We do not address the issue of periodic boundary induced finite-size effects because our motivation here is simply to validate

TABLE II. As for Table I, except that the thermodynamic integration technique is used, and n_b is the number of bins in the g_α distribution.

n_α	n_b	Total MC attempts (10^6)	$\beta\mu$	Time (s)
10	10	200	16.068 ± 0.012	522
10	20	277	16.008 ± 0.013	719
10	30	339	16.027 ± 0.013	897
20	10	206	16.113 ± 0.011	546
20	20	265	16.025 ± 0.012	700
20	30	382	16.028 ± 0.011	1013
30	10	189	16.081 ± 0.012	522
30	20	252	16.002 ± 0.012	700
30	30	336	15.997 ± 0.012	898
40	10	196	16.105 ± 0.013	539
40	20	252	16.031 ± 0.012	683
40	30	364	16.006 ± 0.012	1023

the thermodynamic integration technique proposed above, and this can be achieved by comparison of results with those in paper 2 using a single system size. In any case, these affects were addressed in paper 2 for the hard sphere system.

The perfect (defect-free) fcc hard sphere crystal is simulated at fluid-solid coexistence, so we choose a reduced pressure of $\beta P_s^* = \beta P_s d^3 = 11.487\,24$, where d is the hard sphere diameter (note that in Ref. 34 the reduced coexistence pressure is calculated with an uncertainty of ± 0.09). Temperature is arbitrary for this system. Simulations with $N_s = 108$ are performed (finite-size effects are not investigated here). Results from using parameter hopping (PH) and thermodynamic integration (TI) are compared, where the PH technique is identical to that described in paper 2. The probabilities for choosing each trial move with the TI technique are in the ratio $1:N_s^{-1}$ for displacement and volume moves, respectively. For the PH technique we choose $P_{\alpha_1}^* = 0.555P^*$.

The results for the PH technique are given in Table I, where the length scale $\lambda = d$. This result ($\beta\mu = 16.017 \pm 0.012$) agrees well with that in paper 2 ($\beta\mu = 16.000 \pm 0.014$) despite the clamping error in paper 2 described above, and we take it as our reference point considering that the PH method does not suffer systematic errors due to the choice of n_α (and n_b is irrelevant). As discussed in paper 2, another reference value of $\beta\mu = 15.99 \pm 0.10$ can be obtained from alternative literature sources, although the statistical error in that value is greater than the systematic error caused by finite-size effects. Simulation parameters and results for the TI technique using several values of n_α and n_b are given in Table II. We see that when $n_\alpha \geq 10$ and $n_b \geq 20$ these results agree with the PH result to within 2 standard

TABLE IV. As for Table III except that the thermodynamic integration technique is used and $\alpha_1 = 0.000\,154$.

n_α	n_b	Total MC attempts (10^6)	μ^*	Time (h)
20	20	10.9	-3.208 ± 0.020	0.73

deviations, which is the level of agreement expected for this number of results (only about 1 result in 20 is expected to lie outside of two standard deviations). Results with $n_b = 10$ appear to have significant systematic error. By comparing the time required to obtain PH and TI results to the same level of accuracy, we see that the isothermal-isobaric thermodynamic integration technique is about 40 times more efficient in this case.

For the perfect fcc shifted-force LJ crystal at its triple point, i.e., at a reduced pressure and temperature of $P^* = P\sigma^3/\varepsilon = 0.001\,82$ and $T^* = k_B T/\varepsilon = 0.56$, one result with $N_s = 256$ is obtained (again, finite-size effect is not investigated). For the PH technique we choose $T_{\alpha_1}^* = 1.0$ and $P_{\alpha_1}^* = P^*$. Considering the results for hard spheres, we choose $n_\alpha = 20$ and $n_b = 20$ for the Lennard-Jones case, which should be adequate to within statistical error. As in paper 2, we choose $\alpha_1 = 0.001\,54$ for the PH technique. But for the TI technique this choice might not be adequate, and so instead we choose $\alpha_1 = 0.000\,154$. This illustrates a minor advantage of the PH technique over the TI technique. That is, the replication stage of the PH technique can be used to “jump” to any value of α_1 without loss of accuracy, provided the corresponding system “doubling” Monte Carlo move attempts occur with sufficient probability. But with the TI technique we must choose α_1 to be small enough such that Eq. (8) is accurate. However, this minor advantage is completely outweighed by the efficiency of the TI technique.

Simulation parameters and results are given in Tables III and IV, where this time the length scale $\lambda = \sigma$. This time we find agreement for $\mu^* = \mu/\varepsilon$, to within 2 standard deviations, between the TI result ($\mu^* = -3.208 \pm 0.020$) and the PH result in Table IV ($\mu^* = -3.248 \pm 0.020$), and the result in paper 2 ($\mu^* = -3.204 \pm 0.020$). As discussed in paper 2, another reference value of $\mu^* = -3.23 \pm 0.02$ can be obtained from alternative literature sources for this system. By comparing the time required to obtain PH and TI results to the same level of accuracy, we see that thermodynamic integration is about 320 times more efficient in this case. This suggests that the efficiency gain of the TI technique over the PH technique scales at least with the square of system size [i.e., $320/40 > (256/108)^2$], although we have not performed a detailed analysis.

TABLE III. As for Table I except for the shifted-force Lennard-Jones system, with 256 particles at $P^* = 0.001\,82$, $T^* = 0.56$, $\alpha_1 = 0.001\,54$, and $\alpha_m = 0.138$. μ_{rep}^* and μ_{rel}^* are the replication and relaxation contributions to the total reduced configurational chemical potential μ^* .

n_α	Total MC attempts (10^6)	μ_{rep}^*	μ_{rel}^*	μ^*	Time (hrs)
2000	2159	-0.6743 ± 0.0008	-2.574 ± 0.020	-3.248 ± 0.020	231

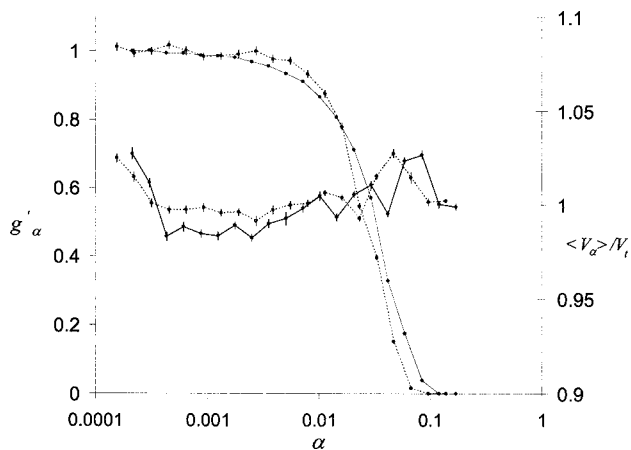


FIG. 1. The variation of g'_α and $\langle V_\alpha \rangle / V_t$ with α for both the hard sphere (solid symbols and lines) and Lennard-Jones (open symbols and dashed lines) fcc crystals (see the text for the meaning of these parameters). Vertical dashes are error bars (to 1 standard deviation), which are shown unless they are smaller than symbols. Lines are a guide to the eye, and α is on a logarithmic scale. $\langle V_\alpha \rangle / V_t$ is always close to 1, while g'_α decreases from near 1 to 0 as α increases.

For both the HS and LJ cases it is useful to examine how $g'_\alpha = \{(4\pi/3)g_\alpha(\alpha L_x, L_x)\alpha^3 L_x^3\}_\alpha$ varies over the chosen range of α to determine whether the chosen limits are sufficient. Figure 1 shows that the limits used are sufficient because this quantity is close to 1 at small α and close to 0 at large α for both systems studied. Also shown is the variation in the system volume relative to the target volume. This shows that the algorithm for controlling the temperature as α varies is adequate.

IV. SUMMARY

In our view, this version of the self-referential method based on thermodynamic integration is the most convenient and efficient method for calculating crystal free energies through molecular simulation yet devised. It is in principle exact (to within statistical error) provided suitable choices of α_1 , α_m , n_α , and n_b are made, it should always avoid problems associated with phase transitions,^{18,26} and it avoids using the grand-canonical ensemble.^{8–15} In terms of convenience, there is no need to evaluate a complicated “center-of-mass” correction or the free energy of a reference crystal,^{3,19,20,27,35,36} or search for optimal parameters for reference states, there is no need to modify the method for hard-core molecules,³ no need to devise optimal paths on a case-by-case basis along integration parameters that avoid phase transitions,²³ and we expect there is no need to “integrate away” pore walls,¹⁶ in the case of confined crystals, for example, so that an integration path that connects with an ideal reference crystal can be defined (although further work is needed to confirm this). Any molecular simulation method that allows configurational Hamiltonians of the form (5) can be used. So in principle molecular dynamics can also be used. It can be employed with either the isothermal-isobaric or canonical ensembles, or equivalent ensembles for confined crystals. We can think of no reason why the choices $P_{\alpha_1} = P_s$ and $\beta_{\alpha_1} = \beta_s/2$, and the algorithm defined by Eq. (29) for traversing the β -path, should not always suffice (note that this al-

gorithm is not needed when using the canonical ensemble route). In this way phase transitions should be avoided. In terms of efficiency, it should be similar to other methods based on thermodynamic integration, such as the lattice coupling expansion method of Frenkel and Ladd²⁰ and Meijer *et al.*²⁷ This work has shown that it is much more efficient than the previous method based on parameter hopping, and we also expect it to be much more efficient than other biased sampling methods.^{2,9,12,22,37} In this work each single-sized system consists of a cubic simulation box, so the double-sized system is a rectangular box. However, because all primary crystal unit cells are parallelepipeds, the SR method should be completely general. Future work will investigate its versatility, by considering molecular crystals, noncubic crystals, and crystals confined within pores.

In this work we only consider the case $n=2m$. Other choices are conceivable, for example, $n_1=1.5n_s$ if there are an even number of unit cells in the simulation box in the direction of \mathbf{L}_x , but they have not been rigorously investigated. A more radical idea that has been mentioned in earlier work² is to set $n_1=n_s+1$ by adapting Tilwani’s retiling idea,⁷ which was formulated in the context of the 2D hard-disk crystal for which the unit cell consists of just one disk. So instead of replicating the entire single-size system to create a double-size system, only a single unit cell (for a bulk crystal) need be replicated. This will dramatically reduce the free energy difference ΔG to be calculated. However, now that thermodynamic integration has been employed in the SR context, it is not clear whether this retiling approach will yield any advantage.

ACKNOWLEDGMENTS

This work is supported by EPSRC Grant No. EP/D034841/1.

- ¹M. B. Sweatman and N. Quirke, *Mol. Simul.* **30**, 23 (2004).
- ²M. B. Sweatman, *Phys. Rev. E* **72**, 016711 (2005).
- ³B. Smit and D. Frenkel, *Understanding Molecular Simulation: From Algorithms to Applications* (Academic, New York, 1996).
- ⁴M. P. Allen and D. J. Tildesley, *Computer Simulation of Liquids* (Clarendon, Oxford, 1987).
- ⁵A. Z. Panagiotopoulos, *Mol. Phys.* **61**, 813 (1987).
- ⁶A. Z. Panagiotopoulos, N. Quirke, M. Stapleton, and D. J. Tildesley, *Mol. Phys.* **63**, 527 (1988).
- ⁷P. Tilwani, “Direct Simulation of Phase Coexistence in Solids using the Gibbs Ensemble: Configuration Annealing Monte Carlo,” Masters thesis, Colorado School of Mines, Golden, 2000.
- ⁸M. Miyahara and K. E. Gubbins, *J. Chem. Phys.* **106**, 2865 (1997).
- ⁹R. Radhakrishnan and K. E. Gubbins, *Mol. Phys.* **96**, 1249 (1999).
- ¹⁰R. Radhakrishnan, K. E. Gubbins, A. Watanabe, and K. Kaneko, *J. Chem. Phys.* **111**, 9058 (1999).
- ¹¹R. Radhakrishnan, K. E. Gubbins, and M. Sliwinska-Bartkowiak, *J. Chem. Phys.* **112**, 11048 (2000).
- ¹²R. Radhakrishnan, K. E. Gubbins, and M. Sliwinska-Bartkowiak, *J. Chem. Phys.* **116**, 1147 (2002).
- ¹³M. Sliwinska-Bartkowiak, J. Gras, R. Sikorski, R. Radhakrishnan, L. Gelb, and K. E. Gubbins, *Langmuir* **15**, 6060 (1999).
- ¹⁴K. G. Ayappa and C. Ghatak, *J. Chem. Phys.* **117**, 5373 (2002).
- ¹⁵C. Ghatak and K. G. Ayappa, *Phys. Rev. E* **64**, 051507 (2001).
- ¹⁶H. Dominguez, M. P. Allen, and R. Evans, *Mol. Phys.* **96**, 209 (1999).
- ¹⁷W. G. Hoover and F. H. Ree, *J. Chem. Phys.* **47**, 4873(1967).
- ¹⁸W. G. Hoover, S. G. Gray, and K. W. Johnson, *J. Chem. Phys.* **55**, 1128 (1978).
- ¹⁹J. Q. Broughton and G. H. Gilmer, *J. Chem. Phys.* **79**, 5095 (1983).
- ²⁰D. Frenkel and A. J. C. Ladd, *J. Chem. Phys.* **81**, 3188 (1984).

- ²¹R. M. Lynden-bell, J. S. van Duijneveldt, and D. Frenkel, *Mol. Phys.* **80**, 801 (1993).
- ²²N. B. Wilding and A. D. Bruce, *Phys. Rev. Lett.* **85**, 5138 (2000).
- ²³G. Grochola, *J. Chem. Phys.* **120**, 2122 (2004).
- ²⁴P. A. Monson and D. A. Kofke, *Adv. Chem. Phys.* **115**, 113 (2000).
- ²⁵J. M. Rickman and R. LeSar, *Annu. Rev. Mater. Res.* **32**, 195 (2002).
- ²⁶W. G. Hoover and F. H. Ree, *J. Chem. Phys.* **47**, 4873 (1967).
- ²⁷E. J. Meijer, D. Frenkel, R. A. Lesar, and A. J. C. Ladd, *J. Chem. Phys.* **92**, 7570 (1990).
- ²⁸C. D. Barnes and D. A. Kofke, *Phys. Rev. E* **65**, 036709 (2002).
- ²⁹K. K. Mon, *Phys. Rev. Lett.* **54**, 2671 (1985).
- ³⁰K. K. Mon and K. Binder, *Phys. Rev. B* **42**, 675 (1990).
- ³¹D. A. Kofke and E. D. Glandt, *Mol. Phys.* **64**, 1105 (1988).
- ³²D. A. Kofke and P. T. Cummings, *Mol. Phys.* **92**, 973 (1997).
- ³³H. Flyvbjerg and H. G. Petersen, *J. Chem. Phys.* **91**, 461 (1989).
- ³⁴N. B. Wilding, *Comput. Phys. Commun.* **146**, 99 (2002).
- ³⁵J. M. Polson, E. Trizac, S. Pronk, and D. Frenkel, *J. Chem. Phys.* **112**, 5339 (2000).
- ³⁶P. D. Beale, *Phys. Rev. E* **66**, 036132 (2002).
- ³⁷J. Chang and S. I. Sandler, *J. Chem. Phys.* **118**, 8390 (2003).